

Experimental Investigation on the Ice Accretion Effects of Airplane Compressor Cascade of Stator Blades on the Aerodynamic Coefficients

M. Ramezanizadeh¹, S. M. H. Pouryoussefi¹, M. Mirzaei^{2†} and S. G. Pouryoussefi²

¹ Air University of Shahid Sattari, Tehran, Iran

² K.N.Toosi University of Technology, Center of Excellence for Design and Simulation of Space Systems, Tehran, Iran

†Corresponding Author Email: mirzaei@kntu.ac.ir

(Received November 12, 2010; accepted January 14, 2012)

ABSTRACT

In this paper the effects of ice accretion on the pressure distribution and the aerodynamic coefficients in a cascade of stator blades were experimentally investigated. Experiments were conducted on stage 67A type stator Controlled-Diffusion blades, which represent the mid-span of the first stage of the stator for a high-bypass turbofan engine. The measurements were carried out over a range of cascade angle of attack from 20° to 45° at Reynolds number of 500000. Experimental blade surface pressure coefficient distribution, lift and drag force coefficients, and momentum coefficients for clean blades were compared with those of the iced blades and the effects of ice accretion on these parameters were discussed. It is observed that the ice accretion on the blades causes the formation of flow bubble on the pressure side, downstream of the leading edge. By increasing the angle of attack from 20° to 35° , the bubble length decreases and the pressure coefficient increases inside the bubble region, constantly. In addition, for the iced blades the diffusion points at the suction side come closer to the trailing edge. In addition, it is found that by increasing the angle of attack up to 35° , the ice accretion has no significant effect on the lift coefficient but the drag coefficient increases comparing with the clean blades. More over at 40° and 45° , by increasing the flow interference effects between the blades, the iced blades experience higher lift and lower drag in comparison with the clean ones.

Keywords: 67A cascade stator blades, Pressure distribution, Iced blade, Airplane engine compressor, Stall conditions.

INTRODUCTION

Inclement weather consideration play an important role in design, analysis, testing and operation of modern high bypass aircraft engines (Venkataramani *et al.* 2007). Since 1990 until 2005, about 240 air crashes have been reported due to the icing in daily flights, which 62 cases were reported as the turbofan engines power loss events. Generally, icing phenomenon occurs at altitudes higher than 22000 ft. in which there is a possibility for existence of super cooled liquid water (Mason *et al.* 2006). Icing creates circumstances in which the super cooled particles of water are accumulated on airframes, engines, propellers and etc. Such accumulation causes the flow disturbance. Mirzaei *et al.* (2009) performed a research using both experimental and numerical approaches on the effects of icing on aerodynamic parameters of NLF-0414 airfoil. It was found that the icing phenomenon on the aerodynamic surfaces such as airplane wing could

decrease lift down to 30% and increase drag up to 40%. While there are many researches done on the effects of icing on wings and airfoils, however, relatively less attention has been paid to the icing effects on the performance of engine inlets, although the effects can be hazardous to engines and aircraft. In particular, ice accretion on the aircraft engine inlet lip can alter the shape of the inlet lip and can cause serious degradation of the performance of an engine inlet (Jin and Taghavi 2008).

Ice accretion downstream the guide vanes could block the air inletting to the engine; this is a stalling circumstance and a serious degradation of the vanes performance. Ice accretion on the booster part of the inlet upstream the guide vanes will decrease the flow rate of inletting core flow and its acceleration. This may cause separation of ice particles and entering the engines, which can damage the mechanical parts downstream, or even stalling the engine or much worse

may cause the engine powerloss during the flight (Mason *et al.* 2006 and Rasmussen *et al.* 2006). On the other hand, ice accretion on the first stage of the stator blades in aircraft engines which are located downstream of the guide vanes, has been recently an interesting subject for researchers. The mechanism of ice accretion on these blades and its aerodynamic and propulsion effects on the engine and the aircraft in general is the base point to investigate this phenomenon. Obtaining the flight certification in the icing condition needs various test flight, which is not only a costly process but also is dangerous. Therefore, it is necessary to simulate this phenomenon experimentally and numerically to provide a useful database and a comprehensive understanding of the effects of ice accretion.

The stator 67A blades which are of the controlled diffusion blades family have been designed by Sanger (1983). Compressor stage 67A was previously studied experimentally and numerically at turbomachinery lab of Naval Postgraduate School by Sanger and Shreeve (1986). Currently, the stage 67A blades are being used in airplane engine compressor blades analysis. These types of blades are used in the compressor first stage of some turbofan engines such as Rolls-Royce 884 Trent and General Electric's GE-90.

Experimental modeling of the shape and geometry of ice accretion especially in cascade on turbomachines has many points and complications. To investigate and analysis the aerodynamic effects of ice accretion, first the ice shape and geometry must be obtained. Since the circumstances of ice formation on the compressor stator blades are very hard to simulate and in flight conditions, these blades are located in the engines, access and having an estimation of the shape and geometry of the ice on the blades is very difficult. LEWICE is one of the comprehensive computer codes for simulation of the phenomenon of icing on airplane designed by NASA.

Ice shapes on airplane engine compressor stage 67A blades were simulated by Lee *et al.* (2006) at the University of Illinois. Moreover, Lee and Lath (2008) extend their work numerically using turbulence modeling by the method of RANS and using LEWICE code. Ice accretion on the blades and its thickness is found to be significantly sensitive to various factors such as droplet size; water contents, ambient temperature and integration time, which all are included in LEWICE code. On the other hand, it is found that the ice shape has weak sensitivity to the inlet flow incident angle and flow turbulence. Figure 1 compares three blades in icing accretion and its thickness simulated by LEWICE software (Lee *et al.* 2006). The blades are in the same conditions except in case (a), the size of droplets, in case (b), the integration time and in case (c), the temperature varies. Pouryoussefi *et al.* (2010) have experimentally surveyed aerodynamic coefficients of 67A stator stage blades. They obtained useful results about the stall condition for the clean blades. Science ice accretion can directly affect the stall conditions of

the blades, an experimental study on icing phenomenon for these types of the blades is needed. In this study, the effects of ice accretion on the pressure coefficient distributions, drag, lift and moment coefficients were experimentally investigated on the stage 67A stator blades. The results of this investigation can provide useful perception of the effects of the ice accretion on the aerodynamic parameters and the performance of the stator blades.

1. EXPERIMENTAL DETAILS

The experiments were conducted in low-speed, open-circuit wind tunnel of aerospace engineering department, K.N. Toosi University of Technology. The wind tunnel test-section is 1.2 m wide, 1 m high and 3 m long. The maximum velocity in the test-section is 65 m/s. under uniform flow conditions, the longitudinal free-stream turbulence intensity is less than 0.2% and the velocity non-uniformity across the test section is $\pm 0.5\%$.

In this study, the experiments were carried out on stage 67A stator blades. For this purpose, three iced blades were used to simulate the two dimensional flow over a cascade of iced stator blades. All of the blades were made of plexiglass which were cut with laser cutter device. The precision of the laser cutter device was ± 0.01 mm and the blade surfaces were finished by painting and polishing: $Ra (\mu m) = 0.05$. Two parallel plates were used at two sides of the cascade span to simulate the two dimensional flow. In addition, all the pressure coefficients distribution and aerodynamic coefficients measurements were performed on the middle blade which was situated between the two other blades. The errors in the spacing and in the alignment of the blades were within $\pm 0.01 C$, where C is the chord length of the blades. For the iced cascade all of the dimensions were the same as the clean cascade whereas ice shape was attached to the blades. The experiments were carried out at Reynolds number of 500000 based on the chord length of a single blade and free stream velocity. Six angles of attack for cascade were investigated ranging from 20° to 45° . Figure 2 shows a schematic view of the cascade of stator blades for clean and iced blades which explains the experimental set-up in the wind tunnel. Moreover, Table 1 illustrates the characteristics of the clean blades and cascade geometry.

The ice shape which was used in the present study was obtained on the 9 min ice accretion for angle of attack of 32.95° deg and for $20 \mu m$ droplets at $-4 F^\circ$ with coupled method in LEWICE (Lee *et al.* 2006). Since, it is found that this type of icing in shape and size have weak sensitivity to the inflow attack angle variations and turbulence around the stage (Lee *et al.* 2006 and Lee and Loth 2008), ice shape was assumed constant in all angles of attack during the experiments. Figure 3 depicts an iced blade which has been formed in such circumstances.

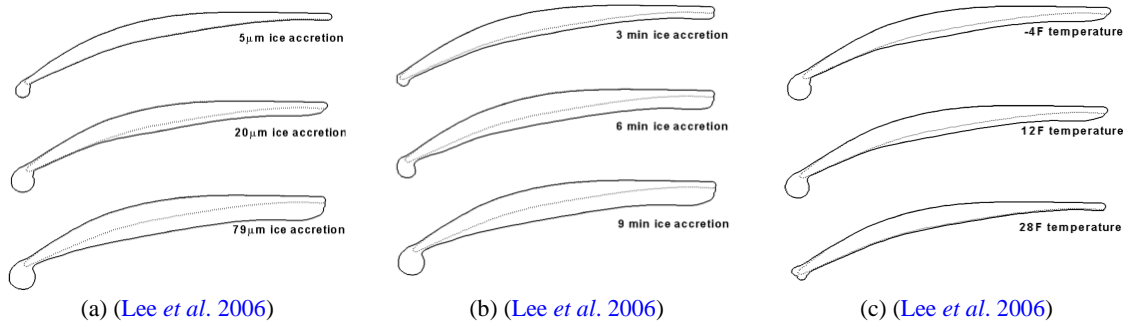


Fig. 1. Ice accretion shapes: (a) for different droplet size; (b) at 3 min intervals; and (c) for different temperatures.

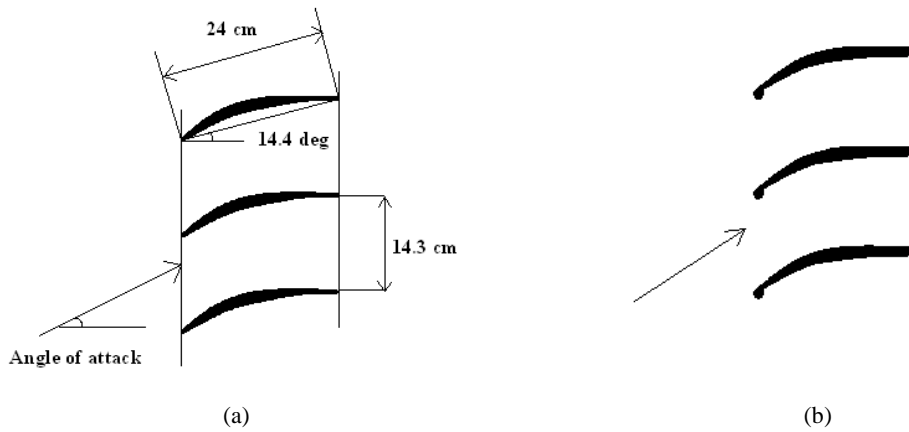


Fig. 2. Schematic view of the cascade of stator blades (experimental set-up in the wind tunnel): (a) clean blades (Pouryoussefi *et al.* 2010); and (b) iced blades

Table 1 The characteristics of the clean blade and cascade geometry. (Stage 67A cascade stator blades)

Camber, deg	41.09
Max thickness, percent chord	7.0
Leading edge radius, percent chord	0.9
Trailing edge radius, percent chord	1.26
Solidity ratio (chord/pitch)	1.67
Stagger angle, deg	14.4
Blade aspect ratio	2
Chord length, cm	24
Blade spacing, cm	14.3
Span length, cm	48

To obtain the surface pressure distribution on the blade, forty pressure taps with inner diameter of 0.5 mm and outer diameter of 1.5 mm are provided (twenty on pressure side and twenty on suction side) in two parallel rows within 1.5 cm distance from each other around the middle blade mid-span in a zigzag manner circumferentially (for both clean and iced blades).

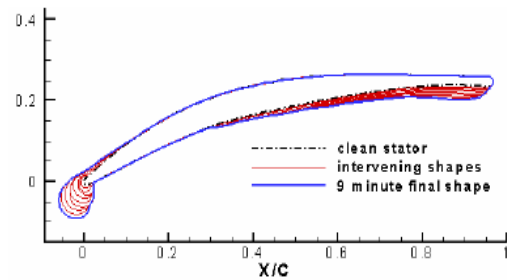


Fig. 3. The ice shape used in the present experiments (Lee *et al.* 2006)

Figure 4 illustrates the pressure tap locations on the surfaces of the clean and iced blades.

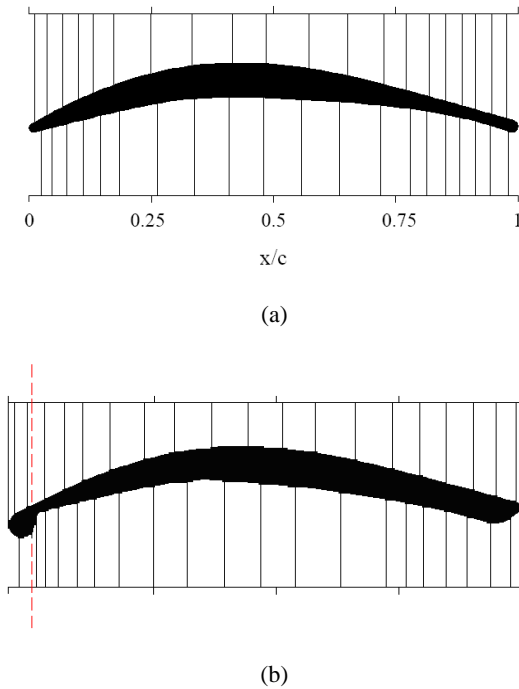


Fig. 4. The pressure taps locations on the surfaces of: (a) clean blade (Pouryoussefi *et al.* 2010); and (b) iced blade

The experiments were accomplished in six different angles of attack: 20° , 25° , 30° , 35° , 40° and 45° . Since for changing the angle of attack, the whole stage of the cascade should rotate, but the test section walls are kept fixed, so we can claim that the inlet flow angle relative to the stage is almost the same as that of the outlet flow and they are parallel to the test section walls. During the experiments, reference flow conditions were measured with a Pitot-static tube and a micro-manometer. On the other hand, the measurement system of the surface pressure was consisted of pressure transducers (Honeywell-DC005NDC4), a National Instruments (NI) PCI-6224 16-bit A/D board with 32 analogue input channels, F.S.S (Farasanjesh) Pressure Field software and a personal computer.

The estimated measurement uncertainties of the pressure, lift, drag and moment coefficients are: $C_p \pm 0.01$, $C_L \pm 0.015$, $C_D \pm 0.02$ and $C_M \pm 0.015$, respectively (the mean aerodynamic coefficients have been measured by pressure distribution method). The pressure coefficient C_p , the lift coefficient C_L , the drag coefficient C_D and the moment coefficient C_M for the blades are defined as

$$C_p = (P - P_\infty) / \left(0.5 \rho V_\infty^2 \right), C_L = L / \left(0.5 \rho V_\infty^2 c \right),$$

$$C_D = D / \left(0.5 \rho V_\infty^2 c \right) \text{ and } C_M = M / \left(0.5 \rho V_\infty^2 c^2 \right)$$

respectively, where P is the mean static pressure on the surface of the blade, P_∞ , the static pressure of the free-stream flow, L , the lift force, D , the drag force, M , the leading edge pitching moment, c , the chord length of the blades, ρ , the air density and V_∞ , the free-stream velocity.

2. RESULTS AND DISCUSSION

As stated previously, for measuring the mean aerodynamic coefficients, the method of pressure distribution was applied using pressure distribution integration around the mid span of the clean and iced blades. Since the blades are high mean camber airfoils and are subjected to high angle of attack, the contribution of friction in drag coefficient is negligible. So, to obtain the drag coefficient, the numerical integration of pressure distribution on the blade surface was used.

To evaluate the validating of the wind tunnel performance and measurement tools, the results have been compared with those of Sanger and Shreeve (1986) in angle of attack of 20° and nearly the same Reynolds number (shown in Fig. 5). A good agreement can be found between their results and those of the present study. There is only a small difference, which may be due to test conditions and instruments precision. Figures 6 to 11 show the pressure coefficient distributions for both clean and iced cascades. Lift, drag and moment coefficients variations for the clean and iced blades vs. angle of attack are shown in Figs. 12 to 14.

3.1 Clean Blades

It is observed that in 20° at the suction side, the pressure coefficient decreases from the leading edge up to $x/c \approx 0.3$ and then gradually increases. The diffusion (divergence) point in the suction side can be found nearly at $x/c = 0.3$ which is the peak of the pressure distribution curve on the suction side. At the pressure side, the pressure coefficient sharply increases from the leading edge up to $x/c \approx 0.4$ and then remains constant with some small fluctuations. On the suction side, the pressure coefficient distribution in 25° approximately has a similar trend of 20° case

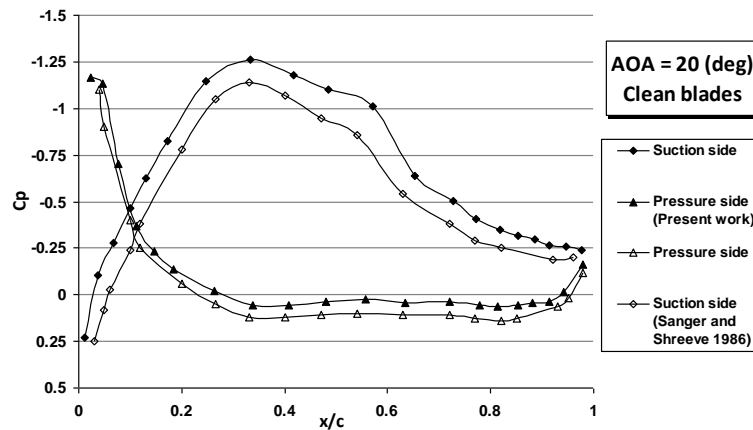


Fig. 5. Comparison of the pressure coefficient distribution with Singer and Shreeve (1986) experimental results

and it can be seen that, the diffusion point is around $x/c=0.3$. In 30° , due to the local suction at the leading edge of the suction side, a pick appears at $x/c \approx 0.05$. In 25° , the pressure coefficient decreases significantly around the leading edge, in comparison with 20° at the suction side and at the pressure side. This causes an increase in difference between the pressure at the suction and the pressure side, by increasing the angle of attack. Such trend continues up to 35° , just before the aerodynamic stall of the clean blades. It is observed that in the range of angle of attack from 20° to 35° , the pressure coefficient at the trailing edge arrives close to -0.25. It is obvious that in 35° in contrary to the lower angle of attack, at the suction side, the diffusion point approaches to the leading edge and the pressure coefficient decreases to -2.75. As it is seen for the pressure distribution at the suction side in 35° , there is a negative constant pressure region from trailing edge to $x/c \approx 0.8$ which shows the occurrence of the separation phenomenon. The movement of the diffusion point at the suction side (which is corresponding to the flow separation at the trailing edge) causes reduction of the performance of cascade in 35° . The pressure distribution of the blades in 35° has significant changed in comparison with those of the lower angles. These variations indicate approaching to the aerodynamic stall for the blades. By increasing the angle of attack, in 40° and 45° , the separation point moves from $x/c=0.8$ to the leading edge and whole the suction surface is exposed to the separation and the pressure coefficient is almost constant. The pressure coefficient distributions for 40° and 45° are almost the same due to stall conditions. The different behavior of the pressure coefficient distribution at the pressure side in these two angles in comparison with the lower angles is due to increasing of the flow interference effect between the blades. Moreover, there is no significant separation region at the pressure side. There

should be more experiments on the pressure distribution in angle of attack ranging from 35° to 40° to have more details about the flow separation region at the suction side.

Figures 12 to 14 illustrate the variations of lift, drag and moment coefficients for the clean and iced blades vs. angle of attack. According to the lift coefficient for the clean blades (Fig. 12), it has linear behavior from 20° to 35° and stall occurs after 35° . In angles from 40° to 45° , the blade has completely stalled. On the other hand, the drag coefficient of the clean blades (Fig. 13) increases before the stall of the blade. An interesting trend of the drag coefficient occurs at angles between 30° to 35° . In this range, the growth rate of the coefficient significantly decreases and this trend changes between 35° and 40° due to stall conditions. Moreover, the variation of moment coefficient (Fig. 14) in the range of 20° to 30° (before blade's stall) is linear but in the angles close to the stall and afterwards, its trend changes and fluctuates around -0.4. Basically, it can be concluded that the lift and drag behavior due to the angle of attack, is almost similar to those of the flow around a 2D airfoil (Mirzaei *et al.* 2009). Whereas, the different moment behavior in comparison with the 2D airfoil can be due to the severe flow interference between the blades at high angles of attack. More study should be done specially on the flow pattern to know the complicated behavior of the aerodynamic coefficients at angles close to the aerodynamic stall.

3.2 Investigation of the Ice Accretion Effects

According to the pressure distribution for the clean blades and iced ones (Figs. 6 to 11), it is observed that in 20° for iced blades, at the suction side, the pressure coefficient decreases from the leading edge to

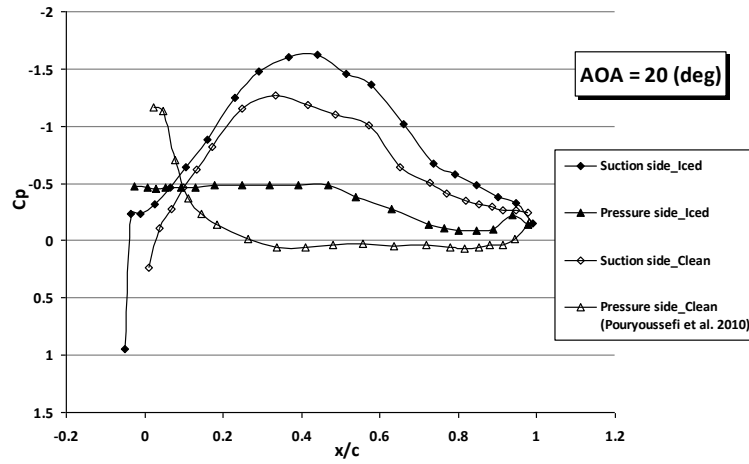


Fig. 6. The pressure coefficient distribution on the blade surface at 20°

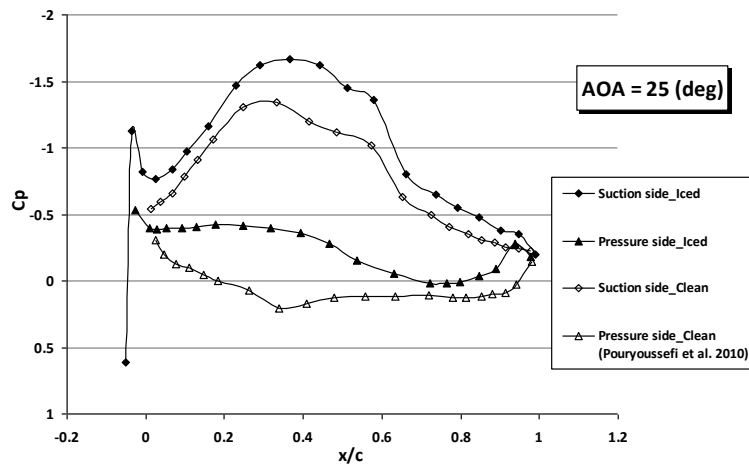


Fig. 7. The pressure coefficient distribution on the blade surface at 25°

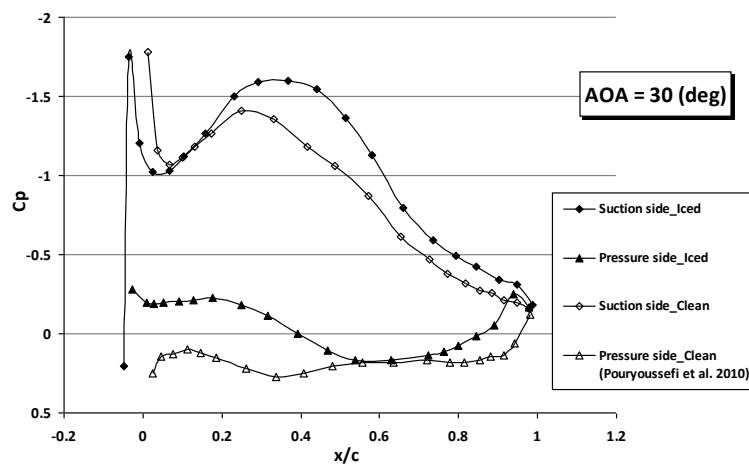


Fig. 8. The pressure coefficient distribution on the blade surface at 30°

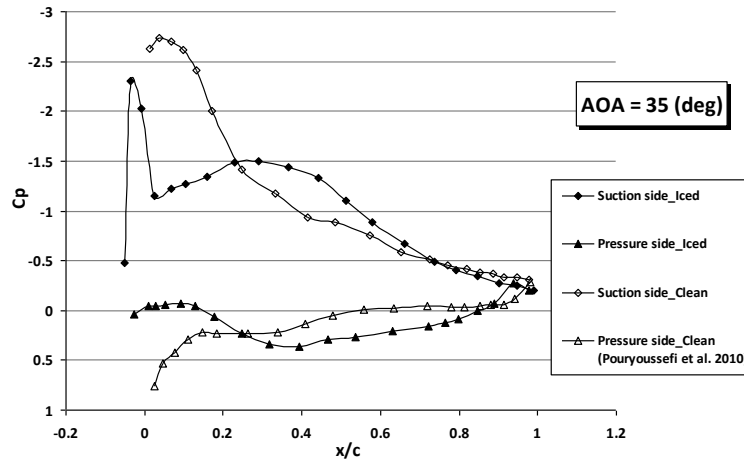


Fig. 9. The pressure coefficient distribution on the blade surface at 35°

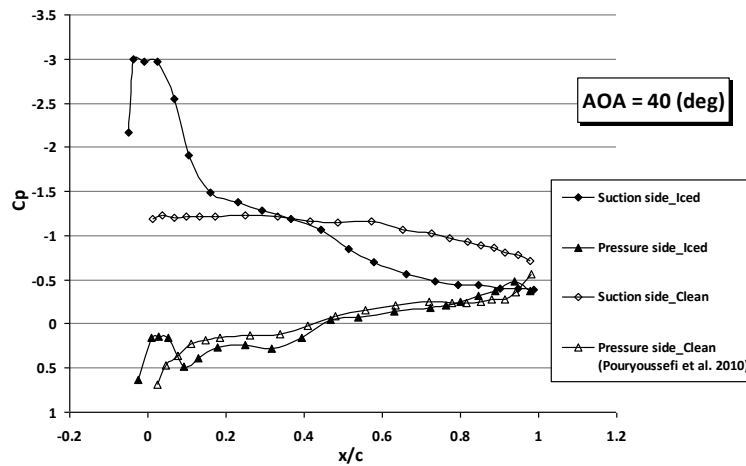


Fig. 10. The pressure coefficient distribution on the blade surface at 40°

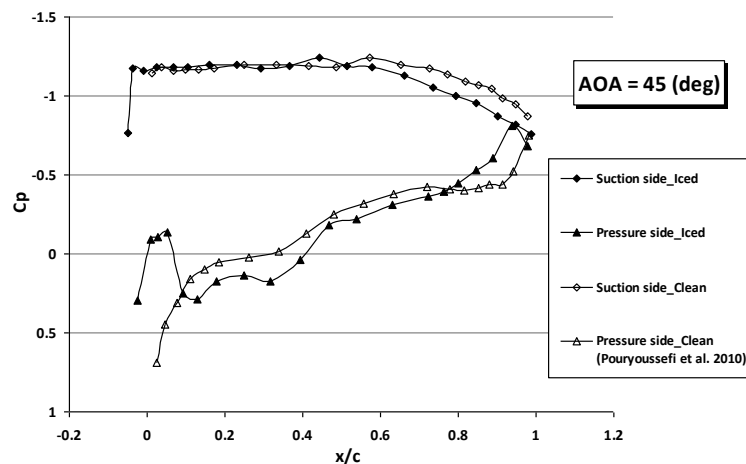


Fig. 11. The pressure coefficient distribution on the blade surface at 45°

$x/c \approx 0.45$ and then recovers. Comparing the clean blades at the same angle of attack, it is found that the diffusion point at the suction side in the iced blades has shifted toward the trailing edge. There is a negative constant pressure region at the pressure side from the leading edge to $x/c \approx 0.5$ which signify the separated bubbles downstream of the iced leading edge and then

the pressure coefficient gradually increases. For 20°, the pressure distribution curve for the iced blade has shifted upward in comparison with that of the clean one, which expresses the iced blades experience less pressure. In 25°, due to the local suction at the suction side of the leading edge, a pick appears for the pressure

curve at $x/c \approx 0.02$. While this pick for clean blades occurs in 30° ; therefore ice accretion causes this pick to appear at lower angle and closer to the leading edge. After the pick, the pressure coefficient decreases up to $x/c \approx 0.45$ (diffusion point) and then increases. For this case, at the pressure side, the separated bubble length downstream the iced leading edge (which is recognized by constant pressure region) has decreased in comparison with 20° for the iced blades and has extended from leading edge to about $x/c = 0.4$. It is also evident that the pressure distribution is shifted upward comparing to the clean blades at the same angle of attack. The major trends for the pressure coefficient distribution in 30° are quite similar to the distribution of 20° and 25° cases. For instance, the bubble length decreases in comparing with 25° and has extended from the leading edge to $x/c \approx 0.2$. By increasing the angle of attack to 35° , a considerable difference appears between the pressure distribution of the clean blades and that of the iced blades. In this angle, the clean blades are close to the aerodynamic stall condition and the diffusion point has shifted toward the leading edge, the separation starts at the trailing edge at the suction side, whereas there is no unexpected phenomenon for the iced blades at this angle of attack. By increasing the angle of attack from 20° to 35° , the separated bubble length decreases and the pressure coefficient increases, continuously. This can be due to the reduction of strength and size of the bubble vortices. In 40° , the pressure coefficient behavior for the iced blades significantly changes comparing to the lower angles due to approaching to stall condition. At the suction side on the iced blades in this angle of attack, the flow separation starts from the trailing edge up to $x/c \approx 0.7$. Moreover, there is no specific diffusion point for the iced blades in this angle. On the other hand, considering the positive sign of the pressure coefficients at the downstream of the iced leading edge at the pressure side, the flow bubble vanishes in 40° . Starting the separation at the suction side and increasing the angle of attack, cause the flow separation area to extend from the trailing edge to the leading edge, in 45° for the iced blades. In this angle, whole the suction side is exposed to the separation. The pressure distributions for the clean and iced blades at the suction side are similar in 45° due to the stall condition. To obtain more details about the separation extension at the suction side, more experiments are needed in the range of 40° to 45° for the iced blades. As pointed before, by increasing the angle of attack the effects of flow interference between the blades increase. Therefore, the pressure distributions at the pressure side in 40° and 45° comparing to the lower angles, experience different behavior.

The variation of lift coefficient vs. angle of attack is shown in Fig. 12. The difference between the clean and iced blades is negligible up to 35° . It is found that at this angle of attack range, the lift coefficient for iced blade is a little bit lower than that of the clean one. While in 40° and 45° , the iced blades experience higher lift coefficient. Considering the lift coefficient,

the clean blade stall occurs at lower angle of attack comparing to the iced blade, in fact icing delays the aerodynamic stall. This phenomenon is due to the blunt ice shape on the leading edge. Figure 13 shows the variation of drag coefficient vs. angle of attack. It can be seen that the drag coefficient of the iced blade is higher than that of the clean one from 20° to 35° . However, for 40° and 45° , the iced blade experiences lower drag coefficient. For iced blade just like the clean one, there is a decrease in the drag coefficient growth rate before stall (from 35° to 40°). This specific behavior (which issues from the flow interference between the blades) appears for the cascaded blades, whereas for the single blade or airfoil, this coefficient and its growth rate continuously increase by increasing the angle of attack. Figure 14 shows that the moment coefficient for both iced and clean blades are approximately equal from 20° to 30° and decreases as the angle of attack increases. According to the leading edge moment coefficient for both clean and iced blades, these values experience little variations in the range of -0.3 to -0.4.

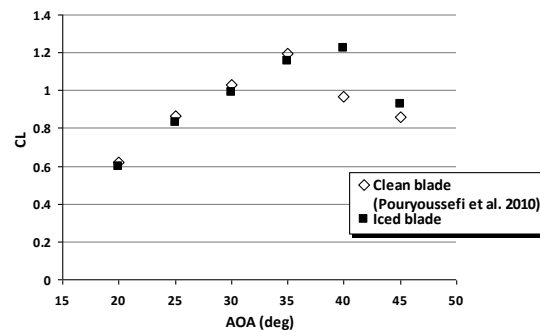


Fig. 12. The lift coefficient variation due to angle of attack changes

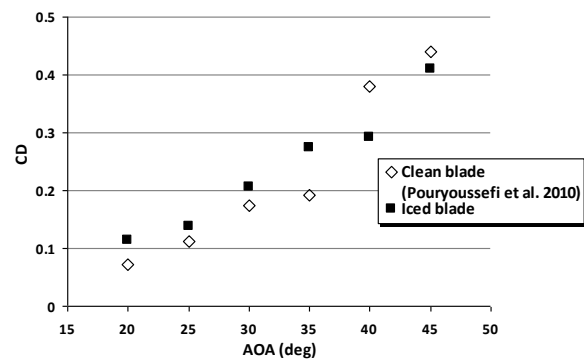


Fig. 13. The drag coefficient variation due to angle of attack changes

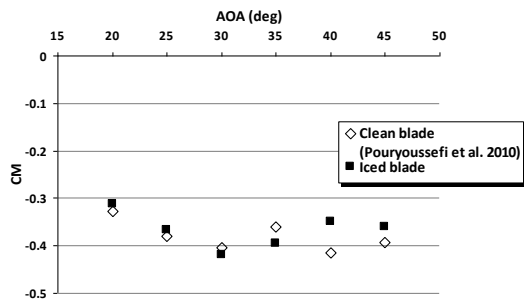


Fig. 14. The moment coefficient variation due to angle of attack changes

3. CONCLUSION

The effects of ice accretion on a 67A type blades cascade which are generally used in the first stator stage of turbofan compressors has been experimentally investigated. The wind tunnel tests were carried out to measure the pressure distribution and the aerodynamic coefficient on the iced blades for six different cascade angle of attack from 20° to 45° at Reynolds number of 500000 and the results were compared with those of the clean ones.

It is found that the angle of attack variations have significant effects on the flow pattern and the aerodynamic coefficients for the clean and iced blades and by increasing the angle of attack, the effects of the flow interference between the blades increase. Moreover, it is concluded that the ice accretion on the blades causes the separated bubble formation at the downstream of the leading edge on the pressure side. It is found that by increasing the angle of attack from 20° to 35° , the separated bubble length decreases and corresponding pressure coefficient increases, constantly. In addition, due to the ice accretion, the diffusion point at the suction side shifts toward the trailing edge. The ice accretion effect on the lift coefficient up to 35° is negligible but causes an increase in the drag coefficient comparing to the clean blades. By increasing the flow interference between the blades in 40° and 45° , the iced blades experience higher lift coefficient and lower drag coefficient in comparison with the clean ones. On the other hand, increasing the angle of attack leads to initiate the flow separation at the suction side and extends the separation region towards the leading edge. The aerodynamic stall for the clean blades occurs in the range of 35° to 40° and for the iced blades, the stall takes place between 40° to 45° . This delay in the blade's stall is due to the blunt ice shape on the leading edge of the blades. Finally, it is suggested that for the analysis and better understanding of the aerodynamic behavior of the cascade of the stator blades, especially in attack angle

close to aerodynamic stall (from 35° to 45°) and also the effects of ice accretion, there should be comprehensive experimental and numerical researches.

REFERENCES

- Jin, W. and R. Taghavi (2008). Computational Study of the Effects of Ice Accretions on the Flow Fields in the M2129 S-Duct Inlets, *AIAA Paper* 08-0075.
- Lee, S., E. Loth, A. Broeren and M. Bragg (2006). Simulation of Icing on a Cascade of Stator Blades, *AIAA Paper* 06-208.
- Lee, S. and E. Loth (2008). Simulation of Icing on a Cascade of Stator Blades, *Journal of Propulsion and Power* 24(6), 1309-1316.
- Mason, J., W. Strapp and P. Chow (2006). The Ice Particle Threat to Engines in Flight, *AIAA Paper* 06-0206.
- Mirzaei, M., M. A. Ardekani and M. Doosttalab (2009). Numerical and experimental study of flow field characteristics of an iced airfoil, *Aerospace Science and Technology* 13(6), 267-276.
- Pouryoussefi, M. H., M. Mirzaei and M. Ramezanizadeh (2010). Experimental Investigation of Pressure Distribution and Aerodynamic Coefficients in a Blade Cascade of an Airplane Engine Compressor, *Journal of Aeronautical Engineering* 12(1), 1-10 (in Persian).
- Rasmussen, R., C. Wade, F. Hage, S. Ladolt, M. Tryhane, J. Cole, A. Ramsay, D. Fleming, R. Moore, A. Davis, B. Reis, T. Lisi, M. Kjolleberg and K. Rosenlund (2006). Ingesting by Jet Engines, *AIAA Journal* 43(5), 1448-1457.
- Sanger, N. L. (1983). The Use of Optimization Techniques to Design Controlled-Diffusion Compressor Blading, *Journal of Engineering for Power* 105, 256-264.
- Sanger, N. L. and R. P. Shreeve (1986). Comparison of Calculated and Experimental Cascade Performance for Controlled-Diffusion Compressor Stator Blading, *Journal of Turbomachinery* 108, 42-50.
- Venkataramani, K., L. McVey, R. Holm and K. Montgomery (2007). Inclement Weather Considerations for Aircraft Engines, *AIAA Paper* 07-0695.